NANO LETTERS

pubs.acs.org/NanoLett

Parametric Amplification and Back-Action Noise Squeezing by a Qubit-Coupled Nanoresonator

Junho Suh,[†] Matthew D. LaHaye,[‡] Pierre M. Echternach,[§] Keith C. Schwab,[||] and Michael L. Roukes*[,†]

[†]Kavli Nanoscience Institute, Condensed Matter Physics, California Institute of Technology, MC 114-36, Pasadena, California 91125, [‡]Department of Physics, Syracuse University, Syracuse New York 13244-1130, [§]Jet Propulsion Laboratory, California Institute of Technology, Pasadena, California 91109, and [||]Applied Physics, California Institute of Technology, MC 128-95, Pasadena, California 91125

ABSTRACT We demonstrate the parametric amplification and noise squeezing of nanomechanical motion utilizing dispersive coupling to a Cooper-pair box qubit. By modulating the qubit bias and resulting mechanical resonance shift, we achieve gain of 30 dB and noise squeezing of 4 dB. This qubit-mediated effect is 3000 times more effective than that resulting from the weak nonlinearity of capacitance to a nearby electrode. This technique may be used to prepare nanomechanical squeezed states.

KEYWORDS NEMS, Cooper-pair-box qubit, dispersive coupling, parametric amplification, noise squeezing, squeezed state

Parametric amplifiers have been essential in manipulating the quantum noise of optical[1−5] and microwave electromagnetic fields.[6−8] At the heart of such experiments, reactive media, including optical crystals, atomic clouds, and Josephson junctions, are strongly driven so that nonlinearities in the media stimulate processes that can be used for signal amplification and vacuum noise squeezing.

Similarly, nonlinearities in micro- and nanoelectromechanical systems (MEMS and NEMS) have been utilized for parametric amplification of motional signals before transduction to the electronic domain,[9−12] including the demonstration of thermal noise squeezing.[12] While several different techniques have been explored for parametric modulation of NEMS and MEMS, the most common approach utilizes the shift in mechanical resonance frequency that results from the electrostatic nonlinearity of a nearby electrode.[12,13]

In principle, parametric modulation via this capacitive "pulling" should enable the preparation of quantum squeezed states of motion.[14] However, due to the microscopic scale of such systems, geometric capacitances are typically very small. Thus, to achieve enough parametric gain to reach the quantum limit or generate quantum squeezed states, large pump amplitudes are required, which could result in deleterious effects that obscure any quantum signatures. For example, assuming the parameters realized in a recent experiment,[15] squeezing the mechanical noise to 10% of the vacuum level would require modulating the gate electrode of the nanoresonator with an amplitude of 300 mV. Operating with such a large pump amplitude could present technical challenges, for example, parasitic coupling to ultrasensitive measurement electronics such as a single-electron transistor or charge qubit.

In contrast, the method that we demonstrate here utilizes the highly nonlinear charge-voltage relationship in a Cooper-pair box (CPB) qubit that results from the Josephson coupling across the CPB's superconducting tunnel junctions. When the nanoresonator is capacitively coupled to the CPB, this charge-voltage relationship affects the nanoresonator's motion and its resonance shows a CPB-state-dependent shift.[16] We find the modulation of the qubit gate voltage produces parametric response of the nanoresonator that is 3000 times greater than what can be achieved using geometric capacitance. Use of the qubit nonlinearity to parametrically pump the nanoresonator also significantly reduces the direct electrostatic drive of the resonator, which occurs simultaneously with the parametric modulation when pumping through geometric capacitance[17] and would further complicate protocols for engineering nonclassical states of the mechanics. Also, such phase-sensitive detection can be utilized for position measurements with sensitivity below the quantum limit for continuous phase-insensitive detection.[18,19] Furthermore, recent theoretical studies[20,21] have shown that a driven CPB can be used as an auxiliary system with which to generate various nonlinear nanomechanical Hamiltonians, opening up the possibility for producing a variety of nonclassical states of nanoresonators.

The effect of the Cooper-pair box (CPB) qubit on the nanoresonator is to shift the mechanical resonance at the lowest order.[22,23] To see this, we assume the nanoresonator to be a simple harmonic oscillator and consider the coupled

* To whom correspondence should be addressed. E-mail: roukes@caltech.edu.
Received for review: 05/25/2010
Published on Web: 09/15/2010

DOI: 10.1021/nl101844r | *Nano Lett.* **2010,** *10,* 3990–3994

Hamiltonian in the qubit charge basis and the harmonic oscillator number basis, using Pauli matrices ($\hat{\sigma}_z$,$\hat{\sigma}_x$) and raising and lowering operators ($\hat{a}^\dagger$,$\hat{a}$):

$$H = 4E_C\left(n_g - \frac{1}{2}\right)\hat{\sigma}_z - \frac{E_J}{2}\hat{\sigma}_x + \hbar\omega_0\left(\hat{a}^\dagger\hat{a} + \frac{1}{2}\right) + \lambda\hat{\sigma}_z(\hat{a}^\dagger + \hat{a}) \tag{1}$$

Here E_C and $E_J = E_{J0}\cos|\Phi/\Phi_0|$ (Φ = flux through the CPB loop, Φ_0 = flux quantum)[24] are the charging and Josephson energies of the qubit respectively, n_g is the gate charge on the CPB in unit of cooper pairs, $\omega_0/2\pi$ is the bare resonance frequency of the nanoresonator, and λ is the coupling strength, given by $\lambda = 4E_c(\partial n_g/\partial x)x_{zp}$, where x = mechanical displacement, $x_{zp} = (\hbar/2m\omega_0)^{1/2}$ and m = effective mass of the nanoresonator. For the parameters of the device measured here, λ is small compared to the other energy scales in the Hamiltonian, and the CPB and nanoresonator are far-detuned (i.e., $\Delta E - \hbar\omega_0 \gg \lambda$). In this dispersive limit, the interaction results in a shift of ω_0 to $\omega_\pm$ that is given by[22,23]

$$\omega_\pm = \omega_0 \pm \frac{2\lambda^2}{\hbar}\frac{E_J^2}{\Delta E(\Delta E^2 - (\hbar\omega_0)^2)} \tag{2}$$

where $\pm$ indicates the qubit is in the excited or ground state, respectively, and $\Delta E = [(4E_c(1 - 2n_g))^2 + E_J^2]^{1/2}$. This state-dependent resonance shift of a harmonic oscillator due to the dispersive interaction with a two-level system is also well-known in various systems such as circuit QED[25,26] and cavity QED.[27]

Degenerate parametric amplification or deamplification is achieved by modulating the resonance shift $\Delta\omega_\pm = \omega_\pm - \omega_0$ at twice of the nanomechanical resonance frequency. From the perspective of the nanoresonator, the shift comes from the change in the effective spring constant (k_{eff}). When the effective spring constant is modulated at twice of its resonance frequency, that is, $k_{eff} = k_0 + \delta k\cos(2\omega_0 t)$, the amplitude of the harmonic oscillator is amplified with respect to that without the parametric modulation (or pump) and the resulting gain G is given by[12]

$$G = \sqrt{\left(\frac{\cos\varphi}{1 + Q\delta\omega/\omega_0}\right)^2 + \left(\frac{\sin\varphi}{1 - Q\delta\omega/\omega_0}\right)^2} \tag{3}$$

where φ is the phase of the force on the resonator at ω_0 relative to the pump and a small δk is assumed ($\delta k/k_0 \approx 2\delta\omega/\omega_0$). When $\varphi = \pi/2$, the gain is maximized and as $\delta\omega \to \omega_0/Q$, the resonator becomes unstable and self-oscillates. On the other hand, when $\varphi = 0$, the gain is minimized and approaches 1/2 as $\delta\omega \to \omega_0/Q$. When the nanoresonator is driven by a random noise force, this deamplification results in noise squeezing.[12]

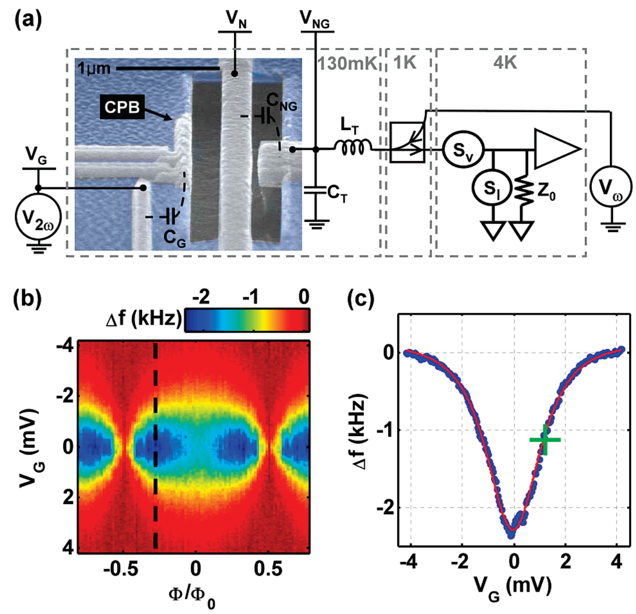

FIGURE 1. Measurement setup and nanomechanical resonance shift due to the interaction with CPB. (a) Scanning electron micrograph of the device and the measurement circuit diagram. The sample picture is colored to show different materials, silicon nitride (blue) and aluminum (gray). The matched cryogenic amplifier (Z_0 = 50 Ω) is modeled to have two uncorrelated sources of noise, S_V for the voltage noise density and S_I for the current noise density. (b) Color map of resonance frequency shift (Δf) versus CPB gate voltage (V_G) and flux (Φ) where Φ_0 is flux quantum. (c) Δf as a function of gate voltage (blue circles), representing the constant-flux cross-section that is indicated in (b) by the vertical dashed line. Red line displays a fit of the data to eq 2. Green cross is the bias point at which parametric response measurements are performed.

The sample micrograph and the measurement circuit are shown in Figure 1a. The nanoresonator is the fundamental in-plane mode of a doubly clamped silicon nitride beam. The resonance frequency of this mode ($\omega_0/2\pi$) is 58.4 MHz. The quality factor of the mode depends on the coupling voltage to the measurement circuit (V_{NG}) and it ranges from 3.8 to 5.8 × 10^4 for V_{NG} = 4 to 8 V. The CPB is connected to the circuit ground by two small Josephson junctions in a DC-SQUID configuration. The charging energy (E_C/h) and the Josephson energy (E_{J0}/h), were determined in a separate spectroscopy measurement to be about 13 GHz.[28]The coupling λ between the nanoresonator and CPB is adjustable by DC voltage V_N and it is 3.2 MHz at V_N = 16 V. The measurement on the nanoresonator is done in an RF reflectometry setup, utilizing a nearby gate electrode to actuate and detect the motion.[29] This is accomplished by applying both a DC bias V_{NG} and an RF bias with frequency near the nanomechanical resonance $\omega \approx \omega_0$. The resulting force on the nanoresonator excites the motion. This in turn generates current across the capacitance between the resonator and the gate (C_{NG}), which is amplified by a cryogenic amplifer at 4 K and then sent to room-temperature electronics for measurement.[28]

DOI: 10.1021/nl101844r | *Nano Lett.* **2010,** *10,* 3990–3994

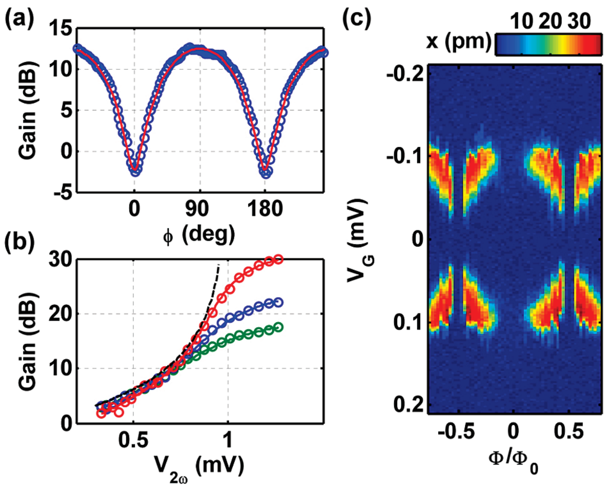

FIGURE 2. Parametric amplification and oscillation. (a) Parametric gain versus phase of the resonator excitation. The blue circles are data taken at $V_{2\omega} = 0.8$ mV and the red line is a fit to eq 3. The amplitude is normalized by the amplitude when $V_{2\omega} = 0$ V and is expressed in dB. (b) Parametric gain versus pump amplitude. From top to bottom, the circles correspond to the measured gains with $V_\omega = 3.6$, 6.3, 11 nV. The black dashed line is a fit to eq 3 with $\varphi = \pi/2$. The solid lines over circles are the fits to eq 4. (c) Map of the parametrically driven resonator amplitude with $V_\omega = 0$ V and $V_{2\omega} = 1.6$ mV, demonstrating self-oscillation in regions of CPB parameter space where the parametric response is maximum.

Figure 1b is the measured resonance shift $\Delta f = (\omega_- - \omega_0)/2\pi$ when the qubit is in the ground state, plotted as a function of the flux Φ applied to the qubit and the qubit gate voltage $V_G = 2q_e n_g/C_G$ (q_e = electron charge). In the map, we pick the constant flux section (dashed vertical line in Figure 1b) where the frequency shift at the charge degeneracy is a maximum. The resulting trace of Δf versus V_G is shown in Figure 1c and fits well to the expected dependence given by eq 2. This fit gives $E_C/h = 12.5$ GHz and $\lambda/h = 3.2$ MHz, which agree respectively with the spectroscopic measurements[28] and an estimate based on finite element simulations (see Supporting Information). To maximize the dynamic range of the parametric pump, we fix V_G so that Δf is half of the value at degeneracy (the bias point is denoted by the green cross in Figure 1c). At this bias point, the parametric pump modulation is given approximately by $\delta\omega/2\pi \approx \partial(\Delta f)/\partial V_G \cdot V_{2\omega}$, where $\partial(\Delta f)/\partial V_G$ is the linear parametric response and $V_{2\omega}$ represents a small modulation of qubit gate bias. From the measured dependence of Δf on V_G, we calculate numerically $\partial(\Delta f)/\partial V_G = 1.1$ kHz/mV. To compare this with the geometric capacitance effect of the qubit gate, we sweep V_G and separately measure the resonance shift without coupling to the qubit ($V_N = 0$ V). We measure $\partial(\Delta f)/\partial V_G = 0.3$ Hz/mV, approximately a factor of 3000 smaller than the parametric response using the CPB.

After setting V_G and Φ, we turn on the resonator excitation $V_\omega \cos(\omega_0 t + \varphi)$ and apply the pump $V_{2\omega}\cos(2\omega_0 t)$ to the CPB gate electrode. Figure 2a shows a typical sweep of nanoresonator amplitude vs φ. A clear periodicity in φ with period π is observed in good agreement with eq 3. In Figure 2b, φ is set at $\pi/2$ and $V_{2\omega}$ is swept for three different values of resonator excitation V_ω. For pump amplitudes up to $V_{2\omega} \cong 0.8$ mV, the data fits well to eq 3 and indicates that the threshold for self-oscillation is 1 mV. Well above this threshold, in Figure 2(c), we clearly observe regions in the qubit parameter space, centered about maxima in $|\partial(\Delta f)/\partial V_G|$, where the nanoresonator becomes unstable and self-oscillates.

It is evident from Figure 2b, that the parametric gain saturates above $V_{2\omega} = 1$ mV. Gain saturation occurs at lower values as the resonator excitation V_ω is increased, occurring at approximately the same mechanical amplitude for each value of V_ω. For pump amplitude $V_{2\omega} = 1.2$ mV, we estimate the saturation amplitude to be $x = 9$ pm. This is much smaller than the critical amplitude for the elastic Duffing nonlinearity,[30] which we estimate to be 1.4 nm. Higher-order terms in the parametric response $\Delta f(V_G)$ are also too small to account for the saturation. We believe that the saturation can be explained by a general model[30-32] that incorporates a nonlinear damping force $\eta x^2 \dot{x}$ on the nanoresonator. Such dissipative effects have been observed in similar parametrically driven mechanical resonators by other groups,[33] and an analogous nonlinear damping is known to exist in superconducting microwave resonators.[34] We use secular perturbation theory[30] to account for the additional nonlinear damping and derive the nanoresonator's amplitude X in response to a harmonic force $F\cos(\omega_0 t)$, finding it to satisfy

$$\frac{\delta k - \delta k_c}{\delta k_c} = \frac{\eta Q \omega_0}{4k_{\text{eff}}} X^2 - \frac{Q}{k_{\text{eff}}} \frac{F}{X} \tag{4}$$

where δk_c is the amplitude of the spring constant modulation at the self-oscillation threshold. From a fit of the data over the full range of $V_{2\omega}$ in Figure 2b to eq 4, we estimate the nonlinear dissipation coefficient to be $\eta \approx 8 \times 10^9$ kg/m^{2}s. This is within an order-of-magnitude of an estimate of $\eta \approx 1 \times 10^9$ kg/m^{2}s, which we calculate numerically from the measured dependence of nanoresonator damping versus qubit gate voltage V_G (see Supporting Information). Further experiments and analysis are necessary to understand the dependence of the resonator damping on qubit gate voltage and the limitations it imposes on the performance of the amplifier.

The phase dependence of a degenerate parametric amplifier can be utilized to deamplify one quadrature component of the input signal and reduce or "squeeze" the noise that accompanies the signal along that quadrature.[12] We demonstrate this effect using our qubit-based parametric amplifier in degenerate mode to squeeze the back-action noise emanating from the capacitive detection circuit onto the nanoresonator. This excess back-action is due to input voltage noise of our cryogenic amplifier (noise temperature ~30 K). With the pump and drive voltage turned off, these

DOI: 10.1021/nl101844r | *Nano Lett.* **2010,** *10,* 3990–3994

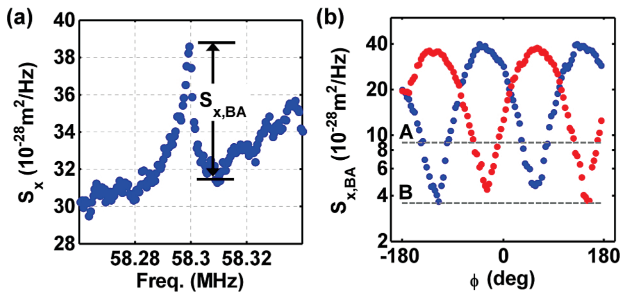

FIGURE 3. Noise measurement and back-action noise squeezing. (a) The noise spectral density of the mechanical displacement with no parametric gain. The slope in the background is due to a slight offset of the nanomechanical resonance from the LC matching frequency. (b) Back-action noise versus reference phase. (blue) *X*-quadrature of the lock-in. (red) *Y*-quadrature. Line "A" is the noise level with no parametric gain and line "B" is at −4 dB from noise level "A".

voltage fluctuations drive the nanoresonator out of equilibrium with the thermal environment at 130 mK to an effective temperature about 8 K given by the peak height ($S_{x,\mathrm{BA}}$) of noise spectrum in Figure 3a (see Supporting Information). With the pump on, we observe the expected squeezing effect using an RF lock-in to monitor both quadratures of the nanoresonator's motion as a function of the reference phase φ, Figure 3b. Deamplification of each quadrature occurs with the expected $\pi/2$ phase difference between quadratures and yields maximum squeezing of 4 dB.

This qubit-based amplification and squeezing technique is the first demonstration of the use of a qubit as an auxiliary system to manipulate the state of nanomechanical motion, albeit classical motion. In future experiments, quantum state engineering of the mechanics will be possible by replacing the present capacitive read-out circuit with a low-loss superconducting microwave resonator (SWR). Through a capacitive coupling of each element to the nanoresonator, independent manipulations of either or both the qubit and SWR could then be used to tailor a specific nanoresonator Hamiltonian.[20] This would enable the production of a large variety of quantum states including vacuum squeezed states and superposition states.

Generating such states would require reducing the thermal occupation number N of the nanomechanical mode close to its quantum ground state (i.e., $k_BT < \hbar\omega_0$). The quantum ground state of a 6 GHz micromechanical resonator was recently demonstrated using conventional dilution refrigeration,[35] and also for a nanoresonator similar to what is described in this paper, $N = 3.8$ has been reached using dynamical back-action cooling from a SWR.[15] With a nanoresonator cooled to low occupation numbers, a vacuum squeezed state of the mechanics could be prepared by utilizing the qubit squeezing technique demonstrated here. Subsequent operations on the qubit applied through a series of microwave pulses could then be used to engineer the nanoresonator interaction Hamiltonian $g(\hat{a}^\dagger\hat{a})^2$ and to generate a superposition of the squeezed states.[20] Implementation of this superposition protocol will require nanoresonator interaction strength g that exceeds both the qubit damping γ and nanoresonator damping Γ. For the present sample, we estimate $g \cong 2$ kHz, $\Gamma = 1.1$ kHz, and $\gamma \cong 1$ GHz.[28] Modifications to the geometry of the sample can yield a factor of at least 10 increase in the electrostatic coupling λ resulting in $g \cong 200$ kHz, which is approaching the lower limit of qubit damping rates demonstrated in circuit-QED, $\gamma < 1$ MHz.[26]

In conclusion, we have demonstrated parametric amplification of nanomechanical motion using the nonlinearity of a driven CPB qubit. The dispersive nanomechanical resonance shift provides significantly more efficient parametric pumping mechanism than existing techniques for nanomechanical parametric modulation. We have performed a proof-of-principle experiment to show that this parametric effect can be used to squeeze nanomechanical motion. Integrating a superconducting microwave resonator with this system should enable the preparation and observation of quantum squeezed states and superposition states of the mechanics.

Acknowledgment. The authors thank to M. Cross, R. Lifshitz and R. Karabalin for discussions and R. E. Muller for electron beam lithography. This research was partially carried out at the Jet Propulsion Laboratory, California Institute of Technology, under a contract with the National Aeronautics and Space Administration.

Supporting Information Available. Model of nonlinear dissipation, amplifier noise model, additional figures, and additional references. This material is available free of charge via the Internet at http://pubs.acs.org.

REFERENCES AND NOTES

(1) Heidmann, A.; Horowicz, R. J.; Reynaud, S.; Giacobino, E.; Fabre, C.; Camy, G. *Phys. Rev. Lett.* **1987**, *59*, 2555.
(2) La Porta, A.; Slusher, R. E.; Yurke, B. *Phys. Rev. Lett.* **1989**, *62*, 28.
(3) Shelby, R. M.; Levenson, M. D.; Perlmutter, S. H.; DeVoe, R. G.; Walls, D. F. *Phys. Rev. Lett.* **1986**, *57*, 691.
(4) Slusher, R. E.; Hollberg, L. W.; Yurke, B.; Mertz, J. C.; Valley, J. F. *Phys. Rev. Lett.* **1985**, *55*, 2409.
(5) Wu, L.-A.; Kimble, H. J.; Hall, J. L.; Wu, H. *Phys. Rev. Lett.* **1986**, *57*, 2520.
(6) Castellanos-Beltran, M. A.; Irwin, K. D.; Hilton, G. C.; Vale, L. R.; Lehnert, K. W. *Nat. Phys.* **2008**, *4*, 929.
(7) Movshovich, R.; Yurke, B.; Kaminsky, P. G.; Smith, A. D.; Silver, A. H.; Simon, R. W.; Schneider, M. V. *Phys. Rev. Lett.* **1990**, *65*, 1419.
(8) Yurke, B.; Kaminsky, P. G.; Miller, R. E.; Whittaker, E. A.; Smith, A. D.; Silver, A. H.; Simon, R. W. *Phys. Rev. Lett.* **1988**, *60*, 764.
(9) Dana, A.; Ho, F.; Yamamoto, Y. *Appl. Phys. Lett.* **1998**, *72*, 1152.
(10) Karabalin, R. B.; Feng, X. L.; Roukes, M. L. *Nano Lett.* **2009**, *9*, 3116.
(11) Mahboob, I.; Yamaguchi, H. *Appl. Phys. Lett.* **2008**, *92*, 173109.
(12) Rugar, D.; Grüter, P. *Phys. Rev. Lett.* **1991**, *67*, 699.
(13) Cleland, A. N.; Roukes, M. L. *Nature* **1998**, *392*, 160.
(14) Blencowe, M. P.; Wybourne, M. N. *Physica B* **2000**, *280*, 555.
(15) Rocheleau, T.; Ndukum, T.; Macklin, C.; Hertzberg, J. B.; Clerk, A. A.; Schwab, K. C. *Nature* **2010**, *463*, 72.
(16) LaHaye, M. D.; Buu, O.; Camarota, B.; Schwab, K. C. *Science* **2004**, *304*, 74.

DOI: 10.1021/nl101844r | *Nano Lett.* **2010,** *10,* 3990–-3994

(17) Cleland, A. N. *Foundations of Nanomechanics*; Springer: New York, 2003.
(18) Caves, C. M. *Phys. Rev. D* **1982**, *26*, 1817.
(19) Clerk, A. A. *Phys. Rev. B* **2004**, *70*, 245306.
(20) Jacobs, K. *Phys. Rev. Lett.* **2007**, *99*, 117203.
(21) Semião, F. L.; Furuya, K.; Milburn, G. J. *Phys. Rev. A* **2009**, *79*, 063811.
(22) Irish, E. K.; Schwab, K. *Phys. Rev. B* **2003**, *68*, 155311.
(23) Zueco, D.; Reuther, G. M.; Kohler, S.; Hänggi, P. *Phys. Rev. A* **2009**, *80*, 033846.
(24) Nakamura, Y.; Pashkin, Y. A.; Tsai, J. S. *Nature* **1999**, *398*, 786.
(25) Schuster, D. I.; Houck, A. A.; Schreier, J. A.; Wallraff, A.; Gambetta, J. M.; Blais, A.; Frunzio, L.; Majer, J.; Johnson, B.; Devoret, M. H.; Girvin, S. M.; Schoelkopf, R. J. *Nature* **2007**, *445*, 515.
(26) Wallraff, A.; Schuster, D. I.; Blais, A.; Frunzio, L.; Huang, R.-S.; Majer, J.; Kumar, S.; Girvin, S. M.; Schoelkopf, R. J. *Nature* **2004**, *431*, 162.
(27) Guerlin, C.; Bernu, J.; Deleglise, S.; Sayrin, C.; Gleyzes, S.; Kuhr, S.; Brune, M.; Raimond, J.-M.; Haroche, S. *Nature* **2007**, *448*, 889.
(28) LaHaye, M. D.; Suh, J.; Echternach, P. M.; Schwab, K. C.; Roukes, M. L. *Nature* **2009**, *459*, 960.
(29) Truitt, P. A.; Hertzberg, J. B.; Huang, C. C.; Ekinci, K. L.; Schwab, K. C. *Nano Lett.* **2007**, *7*, 120.
(30) Lifshitz, R.; Cross, M. C. *Reviews of Nonlinear Dynamics and Complexity*; Wiley-VCH: New York, 2008; Vol. 1.
(31) Lifshitz, R.; Cross, M. C. *Phys. Rev. B* **2003**, *67*, 134302.
(32) Zaitsev, S.; Shtempluck, O.; Buks, E.; Gottlieb, O. 2009, arXiv: 0911.0833 (accessed date of Nov. 12, 2009).
(33) Almog, R.; Zaitsev, S.; Shtempluck, O.; Buks, E. *Phys. Rev. Lett.* **2007**, *98*, 078103.
(34) Yurke, B.; Buks, E. *J. Lightwave Technol.* **2006**, *24*, 5054.
(35) O'Connell, A. D.; Hofheinz, M.; Ansmann, M.; Bialczak, R. C.; Lenander, M.; Lucero, E.; Neeley, M.; Sank, D.; Wang, H.; Weides, M.; Wenner, J.; Martinis, J. M.; Cleland, A. N. *Nature* **2010**, *464*, 697.

DOI: 10.1021/nl101844r | *Nano Lett.* **2010,** *10,* 3990–3994